Analysis on the Dependence of the Fracture Locus on the Pressure and the Lode Angle

Nouira Meriem[1,2], Oliveira Marta[3], Khalfallah Ali[1,4(✉)], Alves José[5], and Menezes Luís[3]

[1] Laboratoire de Génie Mécanique, Ecole Nationale d'Ingénieurs de Monastir, University of Monastir, Av. Ibn El Jazzar, 5019 Monastir, Tunisia
nouirameriem93@gmail.com, ali.khalfallah@gmail.com
[2] Ecole Nationale d'Ingénieurs de Sousse, University of Sousse, 4003 Sousse, Tunisia
[3] Department of Mechanical Engineering, CEMMPRE, University of Coimbra, Polo II Pinhal de Marrocos, 3030-788 Coimbra, Portugal
{marta.oliveira,luis.menezes}@dem.uc.pt
[4] Institut Supérieur des Sciences Appliquées et de Technologie de Sousse, University of Sousse, 4003 Sousse, Tunisia
[5] Department of Mechanical Engineering, CMEMS, University of Minho, Campus de Azurém, 4800-058 Guimarães, Portugal
jlalves@dem.uminho.pt

Abstract. Classical fracture models assume that the stress triaxiality is the key parameter controlling the magnitude of the fracture strain. However, recent works shown the influence of other parameters that characterize the stress state on the prediction of fracture strains. In this work, two uncoupled fracture models, Mae and Wierzbicki [8] and Xue and Wierzbicki [9], were analysed using finite element models. These models define a ductile fracture *locus* formulated in the 3D space of the stress triaxiality, Lode angle parameter and the equivalent fracture strain. The material selected was a cast A356 aluminium alloy for which the model parameters were previously defined. Two groups of tests are analysed in order to provide additional information on the material ductility. The first corresponds to plane strain tests carried out on flat plates with different grooves. The second corresponds to uniaxial tension tests applied on smooth and notched round bars, which were designed with different notch radii. These specimens allow covering a wide range of stress triaxiality. The present work extracts the evolution of the equivalent plastic strain at fracture, the stress triaxiality and the Lode angle parameter in order to evaluate the possibility of using either smooth and notched bars tests or smooth and notched bars tests and grooved plates to evaluate the 3D *locus* for high values of stress triaxiality. In this context, a new function is proposed to describe the equivalent plastic strain at fracture based on the stress triaxiality and the Lode angle parameter.

Keywords: Uncoupled fracture models · 3D fracture *locus* · Equivalent fracture strain · Stress triaxiality · Lode angle

Nomenclature

E	Young's modulus
k	Exponent in curvilinear Lode angle dependence function
m	Damage exponent
n	Strain hardening exponent
p	Mean pressure
p_{lim}	Limiting pressure below which no damage occurs
q	Exponent in pressure dependence function
$\eta = \sigma_m / \sigma_{eq}$	Stress Triaxiality
$\bar{\varepsilon}_f$	Equivalent fracture strain
$\bar{\varepsilon}_{f0}$	Reference equivalent fracture strain
$(\bar{\varepsilon}_{f,t})$	Effective fracture strain under uniaxial tension
$(\bar{\varepsilon}_{f,s})$	Effective fracture strain under pure shear
γ	Ratio of fracture strains
ξ, θ_l	Third invariant of the deviatoric stress tensor, Lode angle
μ_p	Pressure dependence function
μ_θ	Lode angle dependence function
ϑ	Poisson's ratio
$\sigma_{1,2,3}$	Principal components of the Cauchy stress tensor
σ	Cauchy Stress tensor
σ_m	Mean stress
$\sigma_{eq}, \bar{\sigma}$	Equivalent stress
$J_3 = s_1 s_2 s_3$	Is the third stress invariant
D	Damage accumulation
y_0, k and n	Swift law hardening parameters.

1 Introduction

Although it has been extensively studied, the prediction of ductile fracture of metallic materials still presents considerable challenges when resorting to numerical tools to analyse the mechanical behaviour of structural components under various loading conditions. The models proposed in literature for ductile fracture prediction, can be divided in two groups: micromechanical models and continuum damage models. The first relies on the mathematical description of the mechanisms of void nucleation, growth and coalescence. The second group is based on the definition of a damage variable, which acts as a softening mechanism. This type of models can also include phenomenological laws, which can be implemented using a coupled or an uncoupled approach. The Johnson and Cook's uncoupled model [1] integrated the effect of stress triaxiality, strain rate, and temperature [2]. Bao and co-worker [3, 4] designed and performed tests on several type of specimens to calibrate the fracture *locus* in a wide range of stress triaxiality. They showed that the fracture strain does not have to be a monotonically decreasing function of the stress triaxiality [5]. Xue and co-workers [6]

introduced the Lode angle parameter in the definition of the 3D fracture *locus*. This model is similar to the one proposed by Wilkins [7] in the sense that the fracture *locus* is constructed in the 3D space, which defines an equivalent strain to fracture, based on the stress triaxiality and the third invariant of the deviatoric stress tensor.

In this work, the grooved plane strain plates specimens with different notches and tensile tests on smooth and notched round bars will be examined using two uncoupled phenomological fracture models: Mae and Wierzbicki [8] and Xue and Wierzbicki [9].

2   Ductile Fracture Models

A number of ductile fracture models have been proposed to predict failure. In this work, two phenomenological uncoupled models are presented and discussed. They take into account different material parameters to assess the effective fracture strain, for various loading conditions. The mean pressure, the equivalent stress and the stress triaxiality are expressed by the following equations, since the material is assumed to have isotropic plastic behaviour, described by the von Mises yield criterion:

$$p = -\sigma_m = -\frac{1}{3}tr(\sigma) = -\frac{1}{3}(\sigma_1 + \sigma_2 + \sigma_3) \tag{1}$$

$$\bar{\sigma} = \sigma_{eq} = \sqrt{\frac{1}{2}}\sqrt{[(\sigma_1 - \sigma_2)^2 + (\sigma_2 - \sigma_3)^2 + (\sigma_3 - \sigma_1)^2]} \tag{2}$$

$$\eta = -\frac{p}{\sigma_{eq}} = \frac{\sigma_m}{\sigma_{eq}} \tag{3}$$

2.1   Mae and Wierzbicki [8]

Mae and Wierzbicki [8] indicated that the ductile fracture *locus* consists of three branches in the whole range of the stress triaxiality, which define the equivalent strain to fracture ($\bar{\varepsilon}_f$) as follows:

$$\begin{cases} \bar{\varepsilon}_f = \frac{D_1}{1+3\eta}, & -\frac{1}{3} \le \eta \le 0 \\ \bar{\varepsilon}_f = \bar{\varepsilon}_{f,t} + (\bar{\varepsilon}_{f,t} - \bar{\varepsilon}_{f,s})(3\eta - 1), & 0 \le \eta \le \frac{1}{3} \\ \bar{\varepsilon}_f = D_2 e^{D_3\eta} + D_4, & \eta \ge \frac{1}{3} \end{cases} \tag{4}$$

Table 1 Material parameters for ductile fracture characterization of the cast Aluminum Alloy for the model of Mae and Wierzbicki [8]

D1	D2	D3	D4
0.2733	0.1417	−1.545	0.0

where D_1, D_2, D_3, D_4 are the model parameters that must be evaluated for each material. Table 1 presents the parameters determined for a cast aluminium alloy A356, as shown in Mae and Wierzbicki [8].

2.2 Xue and Wierzbicki [9]

Xue and Wierzbicki [9] assume that two other variables play an important role in the evaluation of the equivalent strain to fracture: the mean pressure and the Lode angle (θ_l). The ductile fracture envelope assumes the following form:

$$\overline{\varepsilon_f} = \varepsilon_{f_0}.u_p(p).u_\theta(\theta_l) \tag{5}$$

where the function $u_p(p)$ adopts a logarithmic form:

$$u_p(p) = \begin{cases} 1 - q\log(1 - \frac{p}{p_{\lim}}), & p \geq p_{\lim}(1 - \exp(\frac{1}{q})) \\ 0 & p \leq p_{\lim}(1 - \exp(\frac{1}{q})) \end{cases} \tag{6}$$

and **:

$$u_\theta(\theta_l) = \gamma + (1 - \gamma)(\frac{6\,|\theta_l|}{\pi})^k \tag{7}$$

where $(\theta_l \in [-\frac{\pi}{6}, \frac{\pi}{6}])$. The Lode angle is one of the several parameters that are commonly used to demote the azimuthal angle on an octahedral plane in the principal stress space. It can be defined by:

$$\theta_l = \tan^{-1}(\frac{1}{\sqrt{3}}\frac{2\sigma_2 - \sigma_1 - \sigma_3}{\sigma_1 - \sigma_3}) \quad \text{or by} \quad \theta_l = -\frac{1}{3}\sin^{-1}(\frac{27J_3}{2\overline{\sigma}^3}) \tag{8}$$

$$\xi = \frac{27J_3}{2\overline{\sigma}^3} \tag{9}$$

The parameters $\varepsilon_{f_0}, \gamma, p_{\lim}, q, k, m$ need to be identified for each material. Table 2 presents the set of the parameters determined for an aluminium alloy A356.

Table 2 Material constants for ductile fracture characterization of the cast Aluminum Alloy for the model of Xue and Wierzbicki [9]

ε_{f0}	$p_{\lim}$	q	γ	k	m
1.20	800.0 MPa	1.5	0.6	1.0	1.0

2.3   Damage Evolution

The models previously described define the equivalent plastic strain at fracture in function of the stress state variables used to characterize the stress state. These models allow a direct prediction of the equivalent plastic strain at fracture, for a monotonic stress state. However, when there are changes in the stress path it is necessary to evaluate the impact of those changes in the predicted equivalent plastic strain at fracture. This is commonly done using a damage parameter, D. Ductile failure occurs when the damage parameter reaches the critical damage value of 1.0. The evolution of damage is defined by [9]:

$$D = \int_0^{\varepsilon_c} f(\bar{\varepsilon}_p, \bar{\varepsilon}_f) d\bar{\varepsilon}_p = 1 \tag{10}$$

where ε_c is the equivalent strain at fracture.

For the case of Mae and Wierzbicki [8] model, the damage evolution can be represented by Eq. (11).

$$D = \int_0^{\bar{\varepsilon}^p} \frac{1}{\bar{\varepsilon}_f} d\bar{\varepsilon}_p \tag{11}$$

For Xue and Wierzbicki [9] model, the damage accumulation is expressed in terms of the ratio between the current plastic strain and the equivalent strain to fracture. The damage plasticity model can be represented by the following expressions [9],

$$\dot{D} = m(\frac{\bar{\varepsilon}_p}{\bar{\varepsilon}_f})^{m-1} \frac{\bar{\varepsilon}_p}{\bar{\varepsilon}_f} \tag{12}$$

In this work, the exponent value of damage m is equal to one, i.e. the damage rule corresponds to a linear damage function.

3   Numerical Simulations

Based on the literature review, geometries of standardized and non-standardized test specimens were identified, as shown in Fig. 1. The numerical simulations were performed with the DD3IMPsolver [10, 11]. The commercial software GiD was used as pre and post-processor. Thus, after building the CAD models of the specimens (see Fig. 1), a three-dimensional finite element mesh was built in GID, using eight-node solid finite elements. A selective reduced integration (SRI) technique is employed, with eight and a single GP for the deviatoric and hydrostatic parts of the velocity field gradient, respectively.
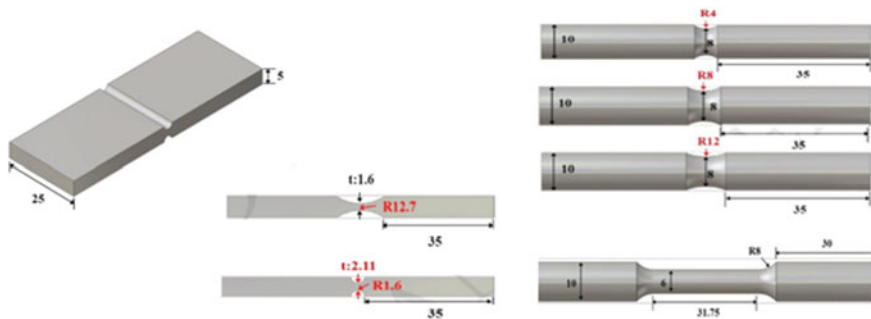
Fig. 1 A sketch of flat-grooved plane strain specimens (left), and smooth and notched round bars specimens [12]

Table 3 Material properties used in the numerical simulation [13]

Material parameters				
Swift law + Linear kinematic hardening			Isotropic elastic behaviour	
y_0	k	n	ϑ	E
200.167	556.06	0.2010	0.33	86 GPa

The numerical simulations were performed considering the two fracture uncoupled models using the cast aluminium alloy. The Swift law (isotropic hardening) is adopted:

$$Y = k(\varepsilon_0 + \bar{\varepsilon})^n \qquad (13)$$

Y represents the yield stress and its evolution during deformation. The initial yield stress y_0 can be written as a function of k, ε_0 and n as follows: $y_0 = k\varepsilon_0^n$. Table 3 present the material parameters.

3.1 Effect of Models Parameters

In this section, the prediction of ductile fracture is analysed for the two groups of classical tests carried out:

- **Flat-grooved Plate Plain Strain Specimens**

Eight different ratio of t/R were considered. All specimens had a constant thickness t = 1.2 and 2.11 mm, respectively at the groove, but the radii of the grooves are equal to 1.6, 4, 8 and 12.7 mm, respectively. The loading condition is simple tension. The notation adopted for these tests is "Tx Rymm", were x is the thickness of the plate and y is the groove radius.

- **Smooth and Notched Round Bars Specimens**

Four values of a/R were assigned to specimens a/R = 0 (smooth round bars), a/R = 1/2, 1 and 2/3 (notched round bars). The notation adopted for theses tests is "R = ymm", were x is the radius of the notch.

   Table 4 summarizes the results obtained with both models. Note that the model proposed by Mae and Wierzbicki [8, 13] only takes the stress triaxiality into account. On the other hand, the model proposed by Xue and Wierzbicki [9] assumes the influence of the mean pressure and the Lode angle. The value of $\bar{\varepsilon}_f$ is the one obtained by the model, assuming a constant value for the variables that characterize the stress state, equal to the one predicted at the onset of ductile fracture. On the other hand, $\bar{\varepsilon}_f^p$ corresponds to the numerically predicted equivalent plastic strain at the location where fracture is predicted by the model. Therefore, the results shown in Table 4 highlight the importance of the damage accumulation variable, since it is clear that there are higher differences between both values when adopting the Xue and Wierzbicki [9] model.

Table 4 A summary of numerical results of fracture strains, stress triaxialities and Lode angle parameters for a cast A356 aluminium alloy

	Tests	$\bar{\varepsilon}_f^p$	$\bar{\varepsilon}_f$	η	θ_l
Mae and Wierzbicki [8]	T1.6 R1.6 mm	0.033	0.032	0.967	−0.05
	T1.6 R4 mm	0.047	0.047	0.713	−0.02
	T1.6 R8 mm	0.054	0.053	0.642	−0.02
	T1.6 R12.7 mm	0.058	0.057	0.597	−0.09
	T2.11 R1.6 mm	0.032	0.031	0.994	−0.13
	T2.11 R4 mm	0.045	0.045	0.747	−0.02
	T2.11 R8 mm	0.053	0.052	0.651	−0.04
	T2.11 R12.7 mm	0.056	0.055	0.614	−0.06
	Smooth round bar	0.085	0.084	0.339	0.999
	R = 4 mm	0.064	0.064	0.519	0.93
	R = 8 mm	0.068	0.067	0.483	0.999
	R = 12 mm	0.073	0.071	0.453	0.999
Xue and Wierzbicki [9]	T1.6 R1.6 mm	0.271	0.182	1.21	−0.01
	T1.6 R4 mm	0.365	0.262	0.996	0.09
	T1.6 R8 mm	0.370	0.281	0.919	0.04
	T1.6 R12.7 mm	0.382	0.288	0.878	0.02
	T2.11 R1.6 mm	0.292	0.223	1.080	0.005
	T2.11 R4 mm	0.349	0.267	0.934	−0.01
	T2.11 R8 mm	0.378	0.298	0.857	0.02
	T2.11 R12.7 mm	0.388	0.296	0.860	0.02
	Smooth round bar	0.673	0.337	0.942	0.996
	R = 4 mm	0.541	0.385	0.929	0.999
	R = 8 mm	0.605	0.478	0.782	0.999
	R = 12 mm	0.647	0.483	0.763	0.999

Although not shown here, this is also related with the fact that the stress triaxiality follows a more stable evolution during the deformation process than the mean pressure and the Lode angle. Also, the mean pressure and the Lode angle evolutions are more sensitive to the mesh descritization adopted.

The analysis of Table 4 also shows that, when considering a tensile loading, all specimens considered present a positive value for the stress triaxiality for the point where ductile fracture is predicted by both models. When considering the Mae and Wierzbicki [8, 13] the flat-grooved plates present a negative value for the Lode angle, while for the Xue and Wierzbicki [9] model, ductile fracture is predicted either for positive or negative values of this parameter. Nevertheless, the Lode angle parameter presents a value close to zero for the flat-grooved plates and a value close to 1.0 for the round bars. Moreover, the Xue and Wierzbicki [9] model is predicting the occurrence of ductile fracture for higher values of tensile displacement, i.e. equivalent plastic strain. Note that this results from the fact that, the parameters shown in Table 2 are recommended by the authors to be used in a coupled implementation of the model, which is not the one adopted in the current work.
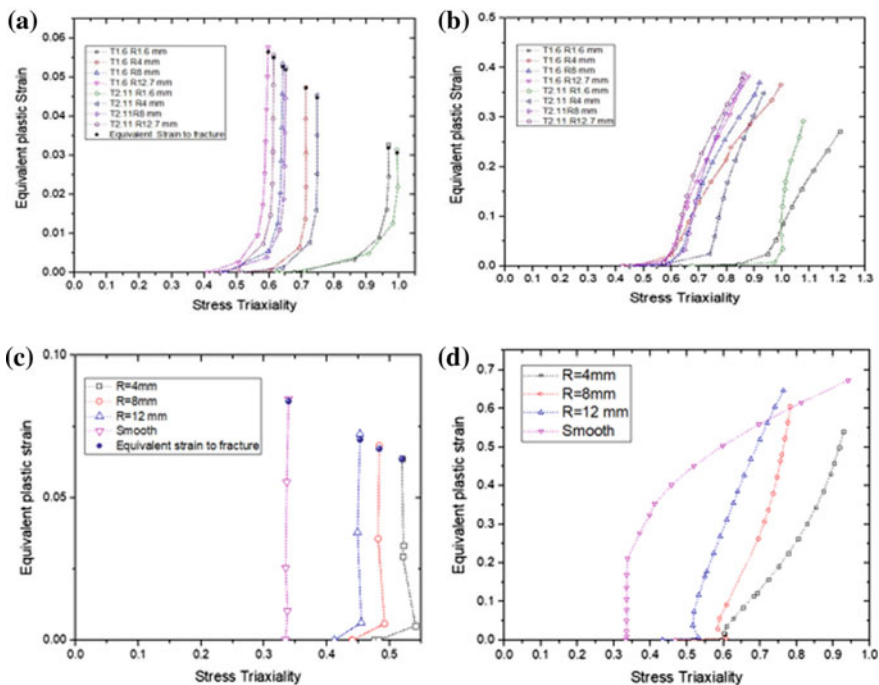

Fig. 2 Equivalent plastic strain versus stress triaxiality in the center of flat-grooved plates (a), (b) and smooth and notched round bars (c), (d) from numerical simulations using the fracture models: a, c Mae and Wierzbicki [8] and b, d Xue and Wierzbicki [9]

Figure 2 shows the evolution of the equivalent plastic strain with the stress triaxiality, obtained for the central element, with the two fracture uncoupled models. Note that the different scale used for both models results from the fact that the Xue and Wierzbicki [9] model always predicts the onset of ductile fracture for much higher values of equivalent plastic strain. The use of uncoupled models always assures that the evolution of the variables that characterize the stress state is equal. The fact that the stress triaxiality suffers an abrupt increase for the central element denotes the onset of necking.
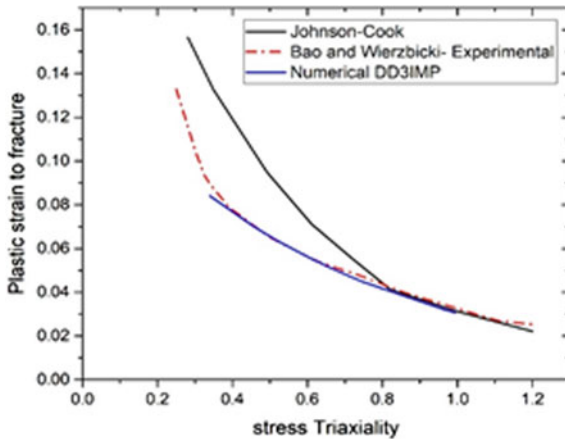

Fig. 3 Fracture loci of the cast Aluminum Alloy [8]

Both Table 4 and Fig. 2 show the effect of stress triaxiality on the predicted fracture strain, under a fixed Lode angle parameter. As the stress triaxiality increases, the equivalent fracture strain and, consequently, the equivalent plastic strain at fracture decreases, for both models. This is an important feature of ductile fracture models as noted by many authors including Johnson-Cook [1]. In fact, theoretical analysis [14, 15] and numerous experimental studies [1, 3, 8, 13] have proved that the fracture strain increases when the stress triaxiality increases. Moreover, since the stress triaxiality is quite constant in the beginning of the tests (see Fig. 2), the damage accumulation follows a linear trend, meaning that the numerically predicted equivalent plastic strain at fracture is almost equal to the one predicted by the the Mae and Wierzbicki model [8]. In fact, as shown in Fig. 3 the results show a good agreement with the experiments performed by Bae and Wierzbicki [8, 16] for the high range of stress triaxiality.

3.2 3D Fracture Locus

Based on the analysis of the results, the two sets of test enable the definition of two boundary limits, for positive values of stress triaxiality:

- $\xi = 0$ corresponding to plane strain, $\bar{\varepsilon}_f^{(0)}$
- $\xi = 1$ corresponding to axial symmetry in deviatoric tension, $\bar{\varepsilon}_f^{(+)}$

This enables the construction of a 3D fracture *locus* that defines the equivalent plastic strain to fracture, based on the stress triaxiality and Lode angle parameter, such as $(\eta, \xi, \bar{\varepsilon}_p^f)$.

If the effect of the Lode angle parameter on the fracture *locus* is neglected, only one set of tests should be considered. In this case, the expression adopted for the range of high values of stress triaxiality is the one corresponding to the third branch of Eq. (4) of Mae and Wierzbicki [8] model, meaning that three parameters need to be identified, D_2, D_3 and D_4. This emplies that a constant surface is assumed for all values of Lode angle parameter. If both sets of tests is considered the effect of the Lode angle parameter is also included. However, based on the analysis of the results, the mean pressure is a variable that with the deformation and is quite sensitive to the mesh discretization adopted. Therefore, a new function is adopted to describe the 3D fracture *locus* for high values of stress triaxiality, as follows [17]:

$$\bar{\varepsilon}_f = D_1 e^{D_2 \eta} - \left(D_1 e^{D_2 \eta} - D_3 e^{D_4 \eta}\right)\left(1 - |\xi|^{\frac{1}{n}}\right)^n \tag{14}$$

In these case five parameters need to be identified, D_1, D_2, D_3 and D_4 and n.

An objective function is chosen in order to minimize the average error between the equivalent plastic strain predicted by the model and the one of each test, as follows:

$$\underset{(D_1, D_2, D_3, D_4)}{Min}(Error) = \underset{(D_1, D_2, D_3, D_4)}{Min} \sum_{i=1}^{N} \left|\bar{\varepsilon}_f, i_{Num} - \bar{\varepsilon}_{f,i\,Calc}\right| \tag{15}$$

where test i listed in Table 4 and N is the total number of tests, $\bar{\varepsilon}_{f,i\,Num}, \bar{\varepsilon}_{f,i\,Calc}$ refer to the numerical determined fracture strain and the calculated fracture strain, respectivelty.

Figure 4 shows the 3D fracture *locus* calibrated using the numerical results obtained with Mae and Wierzbicki [8] model and assuming no influence of the Lode angle parameter. The values obtained for the model parameters are also shown in the Fig. 4. The comparison of the values obtained with the ones used in the numerical simulations (see Table 2) confirms that the optimization procedure recovers the proposed values. This validates the proposed procedure based on the results shown in Fig. 3. Figure 5 shows the 3D fracture *locus* presented in Eq. (14), calibrated using the numerical results obtained with Xue and Wierzbicki [9] model. The set of parameters obtained was the following: $D_1 = 1.9286, D_2 = 1.795, D_3 = 0.9664, D_4 = 1.366$, $n = 0.2$. Moreover, Fig. 5 shows the results for the two boundary limits.

The models previously described define the equivalent plastic strain at fracture in function of the stress state variables used to characterize the stress state. Figures 4 and 5 show a comparison of the 3D surfaces obtained with each model. These surfaces allow a direct prediction of the equivalent plastic strain at fracture, for a monotonic stress state. The calibrated 3D fracture locus can give us a visualized overall view of the models. The shape of the 3D fracture *locus* predicted by Eqs. (4) and (14) are clearly different. In the case of Eq. (4), for $\gamma = 1$, (γ is the ratio of Lode angle function for
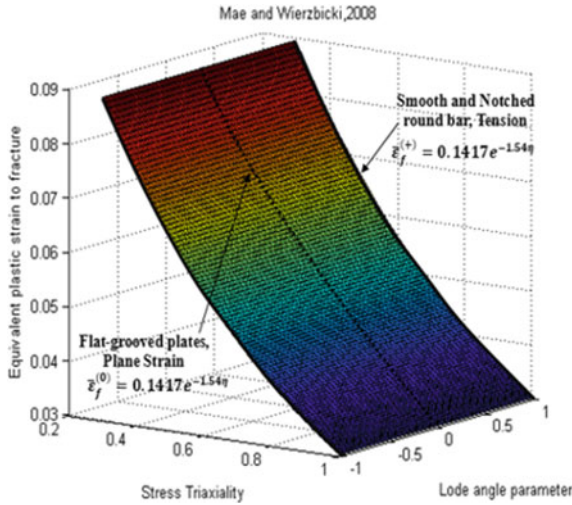
Fig. 4 The 3D Fracture locus of the cast Aluminum Alloy, Mae and Wierzbicki [8]
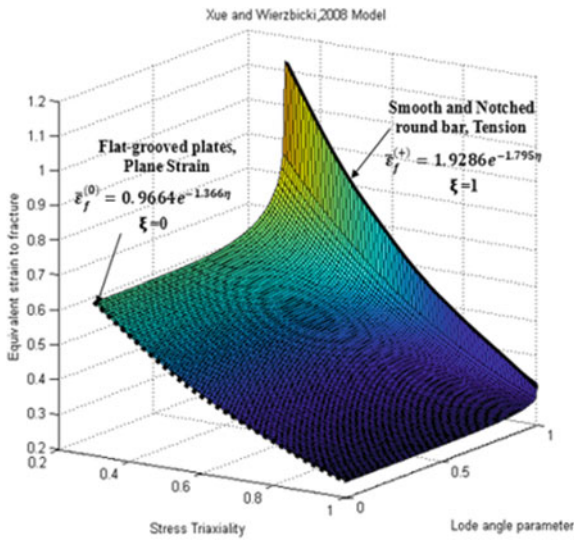

Fig. 5 The 3D Fracture locus of the cast Aluminum Alloy, Xue and Wierzbicki [9]

$\theta_l = 0$ and $\theta_l = -\pi/6$) the predicted fracture locus flattens out and for $0 \prec \gamma \prec 1$, the shape is a concave, similar to that shown in the Xue and Wierzbicki [8, 9, 14], model. Thus, the shape of the 3D fracture locus is sensitive to the Lode angle parameter.

Both models are based on an uncoupled phenomenological approach between fracture and the variables that characterize the stress state; the stress triaxiality, the Lode angle parameter. Therefore, the evolution of the stress and strain distributions is only dictated by the plasticity model adopted and is the same whatever the fracture
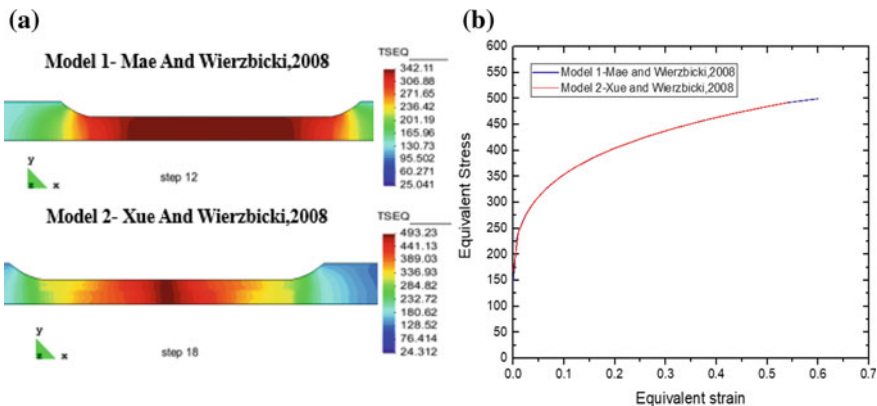
Fig. 6 a The equivalent Stress distribution in specimen, **b** the equivalent Stress versus the equivalent Strain, for the tensile test on smooth round bar

model adopted. This means that fracture strain is predicted for different displacement has a direct result of the fracture locus adopted to analyze the results. Figure 6 indicated that the model adopted, for the tensile test on smooth round bar, has no influence on the stress-strain distribution.

4   Conclusion

In this work two uncoupled models: Mae and Wierzbicki [8] and Xue and Wierzbicki [9], are sued to evaluate the occurrence of ductile fracture, considering two sets pf experimental test. These sets are characterized by presenting a wide range of positive values of stress triaxiality, for two values of Lode angle parameter. The results are used to test a procedure that enables the definition of the fracture *locus*, $(\eta, \xi, \bar{\varepsilon}_p^f)$, following the same approach used by several authors p to construct the fracture *loci* based on experimental results. The results show that the use of tensile tests on round and notched round bars and grooved plates specimens enables the identification of the fracture *locus*, for positive values of stress triaxiality and Lode angle parameter.

References

1. Johnson GR, Cook WH (1985) Fracture characteristics of three metals subjected to various strains, strain rates, temperatures and pressures. Eng Fract Mech 21(1):31–48
2. Teng X, Wierzbicki T (2006) Evaluation of six fracture models in high velocity perforation. Eng Fract Mech 73(12):1653–1678
3. Bao Y (2003) Prediction of ductile crack formation in uncracked bodies. PhD thesis, Massachusetts Institute of Technology, Cambridge
4. Bao Y, Wierzbicki T (2004) On fracture locus in the equivalent strain and stress triaxiality space. Int J Mech Sci 46(1):81–98

5. Bao Y, Wierzbicki T (2005) On the cut-off value of negative triaxiality for fracture. Eng Fract Mech 72(7):1049–1069
6. Bai Y, Wierzbicki T (2008) A new model of metal plasticity and fracture with pressure and lode dependence. Int J Plast 24(6):1071–1096
7. Wilkins ML, Streit RD, Reaugh JE (1980) Cumulative-strain-damage model of ductile fracture: simulation and prediction of engineering fracture tests. Lawrence Livermore Laboratory, Technical Report No. UCRL-53058
8. Teng X, Mae H, Wierzbicki T (2008) Calibration of ductile fracture properties of a cast aluminum alloy. Mater Sci Eng, A 459:156–166
9. Xue L, Wierzbicki T (2008) Damage accumulation and fracture initiation in uncracked ductile solids subject to triaxial loading. Int J Solids Struct 44(16):5163–5181
10. Menezes LF, Teodosiu C (2000) J Mater Process Technol 97:100–106
11. Oliveira MC, Alves JL, Menezes LF (2008) Arch Comput Methods Eng 15:113–162
12. Jinwoo L, Se-Jong K, Daeyong K (2017) Metal plasticity and ductile fracture modeling for cast aluminum alloy parts. J Mater Proc Technol, https://doi.org/10.1016/j.jmatprotec.2017.12.040
13. Mae H, Teng X, Comparison of ductile fracture properties of aluminum castings: Sand mold vs. metal mold. Int J Solids Struct 45:1430–1444
14. Rice JR, Tracey DM (1969) On the ductile enlargement of voids in triaxial stress fields. J Mech Phys Solids 17:201–217
15. McClintock FA (1968) A criterion of ductile fracture by the growth of holes. ASME J Appl Mech 35:363–371
16. Teng X, Wierzbicki T, Bai Y (2008) On the application of stress triaxiality formula for plane strain fracture testing. J Eng Mater Technol https://doi.org/10.1115/1.3078390
17. Antonin P, Jan R, Miroslav S (2013) Identification of ductile damage parameters. In: Simulia community conference